Analytical Modeling of Joule Heating in Electro-Thermal Contacts for Short-Term Industrial Applications

Djillali Benchadli[1], Amina Zemmouri[2*], Salaheddine Azzouz[2,3], Amar Ayad[3], Bourouga Brahim[4]

[1] Faculty of Sciences and Technologies, Higher School of Industrial Technology, Annaba 23000, Algeria
[2] Mechanics of Materials and Plant Maintenance Research Laboratory (LR3MI), Badji Mokhtar University, Annaba 23052, Algeria
[3] Energy Systems Technology Laboratory (LTSE), Higher National School of Technology and Engineering, Annaba 23000, Algeria
[4] LTN-UMR CNRS 6607, E.P.U.N., Rue Christian Pauc, La Chantrerie, Nantes 44306, France

Corresponding Author Email: zemmouri.prfu@gmail.com

ABSTRACT

In industrial processes such as machining, molding, disc brake operation, and spot welding, the thermal transfer at solid-solid interfaces, particularly with heat generation at the interface, is a critical area of study. This research presents a theoretical framework for addressing the direct problem of thermal conduction in electro-thermal contacts, with a focus on short-term scenarios where heat dissipation occurs through the Joule effect. This aspect, not extensively explored in existing literature, is investigated using a semi-analytical method. The study also encompasses a simulation-based exploration, aimed at deepening the understanding of physical phenomena at the contact level. Special attention is given to the thermal transfers initiated at the asperity level of the electro-thermal contact. Findings from this investigation underscore the significance of incorporating the thermal diffusivity of materials into the model for achieving convergence. A notable observation is the increasing divergence over time between the temperatures predicted by numerical and analytical solutions, a trend more pronounced in materials with higher thermal diffusivity, such as titanium. This research contributes valuable insights into the modeling of contact parameters essential for simulating various industrial applications, potentially enhancing efficiency and efficacy in thermal engineering practices.

1. INTRODUCTION

Thermal transfer at solid-to-solid interfaces is of utmost importance in a wide range of industrial applications, including machining, molding, frictional processes, and electrothermal phenomena. Understanding the mechanisms of heat transfer at these interfaces is crucial for optimizing thermal efficiency and improving overall system performance.

Solid-to-solid thermal contacts have been extensively studied to understand the underlying heat transfer mechanisms [1-9]. These studies have delved into various factors, such as contact pressure, material properties, surface characteristics, and interfacial conditions. The insights gained from these investigations have significantly contributed to the development of advanced models and techniques for predicting and optimizing thermal performance. Numerous studies have explored the mechanical aspects of friction interfaces, with temperature being a critical factor that is often highlighted. However, very few studies have modeled and measured this fundamental aspect of sliding contacts. The thermal phenomenon is a dimensioning criterion in many industrial fields, such as the space industry and railways, as friction leads to increased temperatures that can generate degradation of the contact surfaces. Therefore, it is crucial to have a thermal model that represents the sliding interface. Researchers have also explored the impact of heat generation on the thermal resistance of the contact interface, with attention given to understanding the fraction and partition coefficient of the heat flux generated in these systems. These parameters play a crucial role in characterizing the distribution and utilization of heat within the contact interface.

Furthermore, various studies have investigated different aspects of resistance spot welding (RSW) from both experimental and numerical perspectives. For instance, Murugesan et al. [10] investigated the RSW of dissimilar metals, AISI 304 and AISI 316L, and evaluated the ultimate strength and heat utilization of spot welds through finite-element and macrostructural evaluations. Similarly, Hamed Pashazadeh et al. [11] explored the effect of welding parameters on the diameter and height of the nugget using the full factorial design of the experiment methodology. However, electrothermal effects have received relatively less attention in RSW studies, despite their significant influence on the welding process. Electrothermal effects are mainly driven by the current density distribution and the associated Joule heating at the electrode-sheet interface. Feulvarch et al. [12] presented a

general electrothermal contact formulation for RS-WG. Le Meur et al. [13] conducted an experimental study on the electrothermal contact at the electrode-sheet interface during RSW, which showed that the thermal contact resistance and partition coefficient of the generated heat flux vary with time and are affected by current intensity and material conductivity. Later Le Meur et al. [14] developed an experimental methodology to validate the theoretical models of thermal contact resistance and partition coefficient of generated heat flux at the interface. Mokrani and Bourouga [15] conducted an experimental study on the thermal parameters at an imperfect metal-metal contact interface with Joule effect dissipation [16]. The results showed the behavior of these parameters under the influence of contact pressure, materials, and surface states. It has also been suggested to use reverse analysis and experiments [13, 14] to figure out the thermal contact resistance and the partition coefficient of the generated flux. These methods show that these parameters are strongly related. In recent years, several researchers have proposed different approaches to solve electrothermal problems. For instance, Degiovanni et al. [17] proposed an electrical analogy approach to solve heat transfer problems in a system with multiple isotherm surfaces, an exchange surface, and a heat source with any distribution. This method generalizes the concept of thermal resistance and the partition coefficient of the internal heat source. Anas El Maakoul et al. [18, 19] introduced the concept of contact resistance and partition coefficient to describe solid-solid contact with heat sources in electrothermal problems. They found that the partition coefficient is a constant equal to 1/2.

In this study, the analytical framework uses Laplace transforms as a basic tool for dealing with differential equations. These transforms turn the equations that govern heat conduction into the Laplace domain, which makes the problem easier to fully understand. To bridge the gap between the Laplace domain and the temporal domain, the Stehfest numerical inversion method is employed. This method facilitates the conversion of solutions from the Laplace domain back to the temporal domain, offering insights into the temporal evolution of the electrothermal contact system. The entirety of this methodology is referred to as semi-analytical, as it combines analytical techniques with numerical approaches for a comprehensive understanding of electrothermal contact dynamics.

2. SEMI-ANALYTICAL MODEL FOR ELECTRO-THERMAL CONTACT IN SHORT TIME

At short times, thermal disturbances applied to the boundaries only gradually penetrate the medium. Thus, at a relatively short time after the beginning of the phenomenon, the disturbance only reaches a layer of thickness 'e', which is called the penetration depth. Beyond this penetration depth, the rest of the medium has not yet participated in the transient process and is still at its initial condition. Therefore, at this short time interval, the length of the medium has no influence on the behavior of temperature. The assumption of semi-infinite media consists in considering that the length of the medium is infinite.

The chosen model for the electrothermal contact problem involves placing two cylindrical bars of equal circular cross-section in (imperfect) contact across the entirety of their base areas, as shown in Figure 1. The two cylinders are assumed to

be of equal size ($L_1=L_2$ and $D_1=D_2$). This model involves a study in the transient stat, where the imperfect contact creates a thermal contact resistance Rtc. When an electric current passes through the contact, the imperfection of the contact also creates an electrical contact resistance REc. With this passage of electric current, other source terms will appear, such as the heat flux generated at the interface $\varphi g (W/m^2)$ due to the imperfect contact, and the volumetric powers dissipated in the two cylinders P_1 and $P_2 (W/m^2)$. it should be noted that the numerical values used for solving the problem in this study are inspired by the work of Le Meur et al. [13] and have been modified to fit the specific requirements of the electro-thermal contact problem being investigated. Additionally, two temperatures $TL_1=0°C$ and $TL_2=0°C$ are imposed at the left and right boundaries, respectively, and the lateral surface of the two cylinders is assumed to be perfectly insulated.
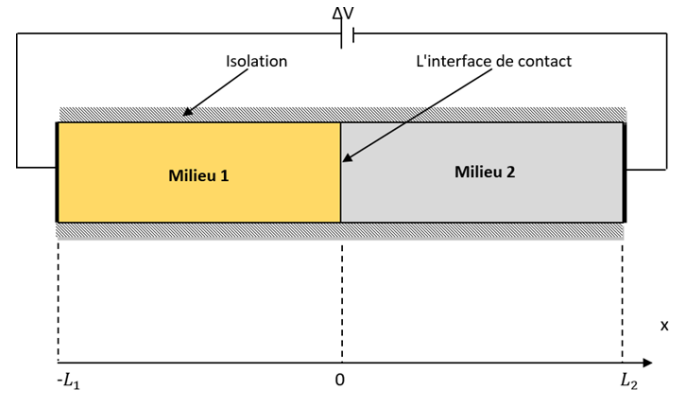

Figure 1. Schematic illustration of the electro-thermal contact model

The literature review [13-16, 18, 19] shows that previous studies have mainly focused on the long-time problem of solid-to-solid thermal contacts, whether for the direct problem or for the estimation and modeling of the parameters of the contact interface with heat generation. They have all investigated the thermal aspect of the macroscopic scale in long-time regimes, but none have looked into the short-time electro-thermal contact problem. This gap in the literature highlights the importance of our study, which aims to investigate the short-time electro-thermal contact problem to contribute to a better understanding of the physical phenomena that occur at the contact interface in these situations.

The model that describes the behavior of electrothermal contact in transient state is presented as follows:

The heat equation in area 1 and 2

$$\begin{cases} \dfrac{\partial^2 T_1}{\partial x^2} + \dfrac{P_1}{\lambda_1} = \dfrac{1}{a_1}\dfrac{\partial T_1}{\partial t} & x \in [-L_1, 0\,] \\[2mm] \dfrac{\partial^2 T_2}{\partial x^2} + \dfrac{P_2}{\lambda_2} = \dfrac{1}{a_2}\dfrac{\partial T_2}{\partial t} & x \in [\,0, L_2\,] \end{cases} \quad (1)$$

Condition at the border

$$x = -L1: \quad T_1(-L_1, t) = T_{-L1}(t) \quad (2)$$

Conservation of the flow at the interface

$$\lambda_1 \frac{\partial T_1(0,t)}{\partial x} = \lambda_2 \frac{\partial T_2(0,t)}{\partial x} + \varphi_g \quad (3)$$

Fourier condition

$$\lambda_2 \frac{\partial T_2(0,t)}{\partial x} + \alpha\varphi_g = \frac{T_2(0,t) - T_1(0,t)}{R_{tc}} \tag{4}$$

Boundary condition at the frontier

$$x = -L1 : \quad T_2(L_2, t) = T_{L_2}(t) \tag{5}$$

The initial condition in area 1 and 2

$$\begin{cases} T_1(x,0) = T_{i_1}(x) \\ T_2(x,0) = T_{i_2}(x) \end{cases} \tag{6}$$

2.1 Application of the transformation to equations

As mentioned above, disturbances during short times primarily impact small thicknesses, justifying the consideration of infinite lengths. However, the system diverges from this norm as the heating associated with volumetric power dissipation extends along the entire length of both cylinders right from the initiation of the phenomenon. To address this unique characteristic, a variable change defined by Eq. (7) is strategically employed:

$$T_j = TP_j + T_{\varphi}j = 1,2 \tag{7}$$

The transformation introduced in the context of the electrothermal contact problem serves to decompose the temperature (T) profiles into two distinct components: where,

TP_j (Volumetric Power Dissipation):
- Captures the temperature increase due to the volumetric powers dissipated in the cylinders during the transient state.
- Associated with the effects of the electric current passing through the contact, resulting in heat generation within the medium.

$T_{\phi j}$ (Generated Flux):
- Represents the temperature increase due to the generated flux at the interface.
- Accounts for the heat flux generated at the imperfect contact interface, contributing to the overall thermal behavior of the system.

Applying the variable change Eq. (7) to the original PDE Eq. (1) yields two transformed expressions:

$$\begin{cases} \dfrac{\partial^2 T_{\varphi j}}{\partial x^2} = \dfrac{1}{a_j} \dfrac{\partial T_{\varphi j}}{\partial t} \\ \dfrac{\partial^2 T_{Pj}}{\partial x^2} + \dfrac{P_j}{\lambda_j} = \dfrac{1}{a_j} \dfrac{\partial T_{Pj}}{\partial t} \end{cases} \tag{8}$$

These transformed equations separate the original PDE into two components: $T_{\phi j}$, related to the generated flux, and TP_j related to the volumetric powers.

2.2 System decomposition

The entire transient state 'A' yields two systems: 'B' and 'C'

- ➢ 'B' representing the heating due to the volumetric powers dissipated in the two cylinders during the transient state, which will be solved over finite lengths;
- ➢ 'C' representing the heating due to the generated flux during the transient stat, which will be solved by considering that both lengths L_1 and L_2 tend towards infinity.

➢ **Case 1: Heating due to volumetric powers (finite lengths)**

2.3 System 'B' - volumetric power dissipation (finite lengths)

System 'B' is designed to analyze the electrothermal contact problem when considering the heating effect due to volumetric power dissipation. The focus is on finite lengths, providing a detailed understanding of temperature profiles in this scenario.

a) Equations for finite lengths

$$\begin{cases} \dfrac{\partial^2 T_{P1}}{\partial x^2} + \dfrac{P_1}{\lambda_1} = \dfrac{1}{a_1} \dfrac{\partial T_{P1}}{\partial t} & x \in [-\infty, 0] \\ \dfrac{\partial^2 T_{P2}}{\partial x^2} + \dfrac{P_2}{\lambda_2} = \dfrac{1}{a_2} \dfrac{\partial T_{P2}}{\partial t} & x \in [0, +\infty] \end{cases} \tag{9}$$

b) Boundary and interface conditions

$$T_{P1}(-L_1, t) = 0 \tag{10}$$

$$\lambda_1 \frac{\partial T_{P1}(0,t)}{\partial x} = \lambda_2 \frac{\partial T_{P2}(0,t)}{\partial x} \tag{11}$$

$$\lambda_2 \frac{\partial T_{P2}(0,t)}{\partial x} = \frac{T_{P2}(0,t) - T_{P1}(0,t)}{R_{tc}} \tag{12}$$

$$T_{P2}(+L_2, t) = 0 \tag{13}$$

$$\begin{cases} T_{P1}(x,0) = 0 \\ T_{P2}(x,0) = 0 \end{cases} \tag{14}$$

c) Solution strategy

The selection of Laplace transforms for solving heat transfer problems in the temporal domain is grounded in the nature of heat conduction equations commonly used in various systems such as welding, non-contact interactions, and more. Heat conduction problems are often formulated as partial differential equations with appropriate boundary conditions that describe the behavior of the system. Laplace transforms have demonstrated significant efficacy in handling linear differential equations, making them particularly well-suited for problems involving heat transfer.

The rationale behind transforming the system from the temporal domain to the Laplace domain lies in the inherent advantages of Laplace transforms in simplifying the mathematical expressions associated with heat conduction. The conversion allows for a more straightforward and systematic analysis of the problem, providing a clear representation of the system's response to electrothermal interactions.

System B undergoes transformation through the application of the Laplace transform, allowing the expression of equations in the Laplace domain. This transformative process significantly simplifies the analysis of transient behavior, resulting in the following solution when applied to Eq. (9):

$$\frac{\partial^2 T_{Pj}}{\partial x^2} - \frac{1}{a_j}\frac{\partial T_{Pj}}{\partial t} = -\frac{P_j}{\lambda_j} \rightarrow \frac{\partial^2 \Theta_{Pj}}{\partial x^2} - \frac{1}{a_j}\left[s.\Theta_{Pj} - T_{Pj}(x,0)\right]$$
$$= -\frac{P_j}{s.\lambda_j}$$

With $T_P(x, 0)=0$ and 's' the Laplace variable.

$$\begin{cases} \dfrac{\partial^2 \Theta_{P1}}{\partial x^2} - \dfrac{s}{a_1}\Theta_{P1} = -\dfrac{P_1}{\lambda_1}.s^{-1} \\ \dfrac{\partial^2 \Theta_{P2}}{\partial x^2} - \dfrac{s}{a_2}\Theta_{P2} = -\dfrac{P_2}{\lambda_2}.s^{-1} \end{cases} \quad (15)$$

The solutions for the transformed Eq. (15) are detailed as follows:

$$\begin{cases} \Theta_{P1}(x,s) = C_1 e^{-q_1 x} + C_2 e^{+q_1 x} + \dfrac{a_1 P_1}{\lambda_1}.s^{-2} \\ \Theta_{P2}(x,s) = C_3 e^{-q_2 x} + C_4 e^{+q_2 x} + \dfrac{a_2 P_2}{\lambda_2}.s^{-2} \end{cases} \quad (16)$$

d) Numerical inversion

The Stehfest method [20] is employed for numerical inversion in the Laplace domain due to the unconventional nature of the temperature field solution. The solution obtained in the Laplace domain doesn't conform to standard functions, making direct inversion using traditional methods challenging. The Stehfest method is chosen for its proven effectiveness in handling such non-standard functions, offering a reliable and efficient approach to invert the Laplace-transformed equations. Its application ensures accurate insights into the temporal evolution of the electrothermal contact system, addressing the specific complexities associated with the analytical framework utilized in this study.

The solutions for the transformed Eq. (16) involve coefficients C_1, C_2, C_3 and C_4, which are determined by applying boundary conditions. These coefficients play a crucial role in shaping the behavior of the system during the transient state.

To execute the inversion from $\theta_{P1}(x,s) \rightarrow T_{P1}(x,t)$, the Stehfest numerical inversion method is applied. This involves calculating $T_{Pj}(x,t)$ using the formula:

$$T_{Pj}(x,t) = \left(\frac{\ln(2)}{t}\right)\sum_{j=1}^{N} V_j(N)\ \Theta_{Pj}\left(j\frac{\ln(2)}{t}\right) \quad (17)$$

The term V_j is computed using the given formula:

$$V_j = (-1)^{\frac{N}{2}+j}\sum_{k=\lfloor\frac{j+1}{2}\rfloor}^{min\left(i,\frac{N}{2}\right)}\frac{k^{\frac{N}{2}}(2k)!}{\left(\frac{N}{2}-k\right)!\,k!\,(k-1)!\,(j-k)!\,(2k-j)!} \quad (18)$$

Setting N=10 in the Stehfest numerical inversion method strikes a balance between computational efficiency and precision. This choice, representing single precision, is a standard compromise for numerical simulations, offering satisfactory results for various engineering applications. It reflects a pragmatic decision, acknowledging the diminishing returns in accuracy with higher N values while ensuring manageable computational demands for the electrothermal contact problem under consideration.

➢ **Case 2: Heating due to the generated flow**

2.4 System 'C' - generated flow (infinite lengths)

The system 'C' of equations is established to describe the thermal behavior in scenarios where the generated flow influences the entire length. The partial differential equations (PDEs) under consideration are expressed in terms of temperature profiles and their spatial and temporal derivatives.

a) Equations for infinite lengths

$$\begin{cases} \dfrac{\partial^2 T_{\varphi1}}{\partial x^2} = \dfrac{1}{a_1}\dfrac{\partial T_{\varphi1}}{\partial t} & x \in [-\infty, 0] \\ \dfrac{\partial^2 T_{\varphi2}}{\partial x^2} = \dfrac{1}{a_2}\dfrac{\partial T_{\varphi2}}{\partial t} & x \in [0, +\infty] \end{cases} \quad (19)$$

b) Boundary and interface conditions

The set of conditions for System 'C' includes initial and boundary conditions that ensure the physical relevance of the solution.

$$T_{\varphi1}(x \rightarrow -\infty, t) = 0 \quad (20)$$

$$\lambda_1\frac{\partial T_{\varphi1}(0,t)}{\partial x} = \lambda_2\frac{\partial T_{\varphi2}(0,t)}{\partial x} + \varphi_g \quad (21)$$

$$\lambda_2\frac{\partial T_{\varphi2}(0,t)}{\partial x} + \alpha\varphi_g = \frac{T_{\varphi2}(0,t) - T_{\varphi1}(0,t)}{R_{tc}} \quad (22)$$

$$T_{\varphi2}(x \rightarrow +\infty, t) = 0 \quad (23)$$

$$\begin{cases} T_{\varphi1}(x,0) = 0 \\ T_{\varphi2}(x,0) = 0 \end{cases} \quad (24)$$

c) Solution strategy

By applying the Laplace transform to Eq. (19), the resulting expression is:

$$\rightarrow \frac{\partial^2 \Theta_{\varphi1}}{\partial x^2} - \frac{s}{a_1}\Theta_{\varphi1}(x,s) = 0 \rightarrow \Theta_{\varphi1}(x,s)$$
$$= C_1 e^{-q_1 x} + C_2 e^{+q_1 x}\ With\ q_1 = \sqrt{\frac{s}{a_1}}$$

$$\rightarrow \frac{\partial^2 \Theta_{\varphi2}}{\partial x^2} - \frac{s}{a_2}\Theta_{\varphi2}(x,s) = 0 \rightarrow \Theta_{\varphi2}(x,s)$$
$$= C_3 e^{-q_2 x} + C_4 e^{+q_2 x}\ With\ q_2 = \sqrt{\frac{s}{a_2}}$$

When x tends to $-\infty$ the temperature reaches a finite value which implies that C_1=0.

When x tends to $+\infty$ the temperature reaches a finite value which implies that $C_4=0$.

$$\begin{cases} \Theta_{P1}(x,s) = A_1 e^{+q_1 x} \\ \qquad . \\ \Theta_{P2}(x,s) = A_2 e^{-q_2 x} \end{cases} \qquad (25)$$

d) Numerical inversion

The coefficients (A_1 and A_2) are determined by applying boundary conditions to ensure a physically meaningful solution.

$$A_2 = \frac{\varphi_g \left(E_1 R_{tc}\, \alpha.\, s^{-\frac{1}{2}} + 1 \right)}{R_{tc}\, E_1 E_2.\, s + (E_1 + E_2).\, s^{-\frac{1}{2}}}.\, s^{-1} \qquad (26)$$

$$A_1 = \frac{\varphi_g.\, s^{-2}.\, (\alpha R_{tc}{}^2 E_1 E_2 + E_1 R_{tc}\, \alpha + R_{tc}\, E_2) + \varphi_g.\, s^{-1}.\, (1 - R_{tc}\, \alpha)}{R_{tc}\, E_1 E_2.\, s + (E_1 + E_2).\, s^{-\frac{1}{2}}} \qquad (27)$$

With:
E: thermal effusivity $E_j = \sqrt{\lambda_j c_j \rho_j}$

Numerical inversion was used by the Stehfest method, as mentioned earlier since there was no way for an analytic inversion.

2.5 System 'D' - Generated Flow (Finite Lengths)

System 'D' extends the analysis of the electrothermal contact problem in the presence of the generated flow, focusing on finite lengths. It provides insights into the system's behavior when considering the influence of the generated flux within specific length constraints.

a) Equations for infinite lengths

$$\begin{cases} \dfrac{\partial^2 T_{\varphi 1}}{\partial x^2} = \dfrac{1}{a_1} \dfrac{\partial T_{\varphi 1}}{\partial t} & x \in [-L_1, 0] \\[2mm] \dfrac{\partial^2 T_{\varphi 2}}{\partial x^2} = \dfrac{1}{a_2} \dfrac{\partial T_{\varphi 2}}{\partial t} & x \in [\,0, L_2] \end{cases} \qquad (28)$$

b) Boundary and interface conditions

$$T_{\varphi 1}(-L_1, t) = 0 \qquad (29)$$

$$\lambda_1 \frac{\partial T_{\varphi 1}(0,t)}{\partial x} = \lambda_2 \frac{\partial T_{\varphi 2}(0,t)}{\partial x} + \varphi_g \qquad (30)$$

$$\lambda_2 \frac{\partial T_{\varphi 2}(0,t)}{\partial x} + \alpha \varphi_g = \frac{T_{\varphi 2}(0,t) - T_{\varphi 1}(0,t)}{R_{tc}} \qquad (31)$$

$$T_{\varphi 2}(L_2, t) = 0 \qquad (32)$$

$$\begin{cases} T_{\varphi 1}(x,0) = 0 \\ T_{\varphi 2}(x,0) = 0 \end{cases} \qquad (33)$$

c) Solution strategy

By applying the Laplace transform to Eq. (28), the transformed equation is obtained as follows:

$$\rightarrow \frac{\partial^2 \Theta_{\varphi 1}}{\partial x^2} - \frac{s}{a_1} \Theta_{\varphi 1}(x,s) = 0 \rightarrow \Theta_{\varphi 1}(x,s)$$

$$= A_1 e^{q_1 x} + A_2 e^{-q_1 x} \; With \; q_1 = \sqrt{\frac{s}{a_1}}$$

$$\rightarrow \frac{\partial^2 \Theta_{\varphi 2}}{\partial x^2} - \frac{s}{a_2} \Theta_{\varphi 2}(x,s) = 0 \rightarrow \Theta_{\varphi 2}(x,s)$$

$$= B_1 e^{q_2 x} + B_2 e^{-q_2 x} \; With \; q_2 = \sqrt{\frac{s}{a_2}}$$

d) Numerical inversion

The A_i and B_i coefficients are found by applying boundary conditions, solving the following matrix system:

$$\begin{pmatrix} e^{-q_1 L_1} & e^{q_1 L_1} & 0 & 0 \\ 0 & 0 & e^{q_2 L_2} & e^{-q_2 L_2} \\ q_1 \lambda_1 & -q_1 \lambda_1 & -q_2 \lambda_2 & q_2 \lambda_2 \\ 1 & 1 & (q_2 \lambda_2 R_{tc} - 1) & -(q_2 \lambda_2 R_{tc} + 1) \end{pmatrix} \times \begin{pmatrix} A_1 \\ A_2 \\ B_1 \\ B_2 \end{pmatrix}$$

$$= \begin{pmatrix} T_{L1} \\ T_{L2} \\ \dfrac{\varphi_g}{s} \\ -\alpha \varphi_g\, R_{tc}\, \boldsymbol{s^{-1}} \end{pmatrix}$$

The analytical framework employed plays a pivotal role in elucidating the temperature field or distribution during electrothermal contact. This, in turn, facilitates the assessment of key parameters that govern heat transfer in such contact scenarios. The results derived from the analytical model, manifesting as temperature profiles or distributions, offer a comprehensive depiction of the thermal behavior within the system.

A detailed analysis of these results provides valuable insights into the distribution, propagation, and dissipation of heat during electrothermal contact. The temperature profiles allow for a nuanced understanding of transient behavior, showcasing variations at different time intervals and positions within the contact interface.

Furthermore, interpreting these results contributes to a better understanding of how various factors, such as material properties, contact resistance, and generated heat flux, impact the overall thermal performance. This interpretation enables the identification of patterns, critical points, and an evaluation of the effectiveness of electrothermal contact under different conditions.

3. RESULTS AND DISCUSSION

In the course of this study, meticulous numerical simulations were conducted using the COMSOL software, renowned for its efficiency in analyzing complex phenomena, especially those involving electrical and thermal considerations. The investigation involves two distinct cases.

For each case, specific parameters were rigorously defined, including geometry and meshing, material properties, thermal and electrical boundary conditions, as well as multiphysical coupling in the COMSOL interface. Regarding thermal boundary conditions, prescribed temperatures at the ends of the bars and the thermal contact resistance at the interface, notably through the introduction of a contact resistance based on the Yovanovitch model [21], were carefully specified. In parallel, electrical boundary conditions involved applying a voltage at one end of the bars.

Multiphysical coupling was achieved using the appropriate interface in COMSOL, allowing for a coherent integration of heat transfer equations with electrical current equations. Volumetric power generation due to electrical current was incorporated as a coupling term, with parameters tailored to each case.

Furthermore, comprehensive temporal studies were conducted to capture the transient behavior of electrothermal contact. This approach underscores the commitment to a thorough analysis of the phenomenon, providing crucial insights into the understanding of complex interactions at the electrothermal contact interface.

The choice of materials for this study is Titanium/Aluminum, which have been selected based on their physical properties presented in Table 1. With an electric current of $I=300A$ and a thermal contact resistance of $Rtc=1.8\times10^{-3}$ ($K.m^2/W$), these materials have been found to yield good agreement between the results obtained using both the Comsol model and the semi-analytical solution. Furthermore, the unique characteristics of Titanium and Aluminum make them particularly well-suited for electrothermal applications. Titanium is a high-strength, lightweight metal with excellent corrosion resistance and good thermal conductivity. Aluminum is also lightweight, with good thermal and electrical conductivity. Additionally, it has a low melting point, which makes it easy to shape and form.

Table 1. Physical characteristics of the utilized materials

	Titanium	Aluminum
D(mm)	30	30
L(Mm)	60	60
λ(W/m.K)	21.9	155
ρ(Kg/m³)	4506	2730
Cp(J/kg.K)	522	893
σ(Ω⁻¹m⁻¹)	2.6 106	2,326 107

In this section, the results obtained for two different cases of heating in electrothermal contacts will be presented.

- The first case involves heating due to volumetric powers with finite lengths,
- The second case focuses on heating due to the generated flow with infinite lengths.

The analysis of these cases provides valuable insights into the heat transfer characteristics and behavior of the materials involved in electrothermal contact.

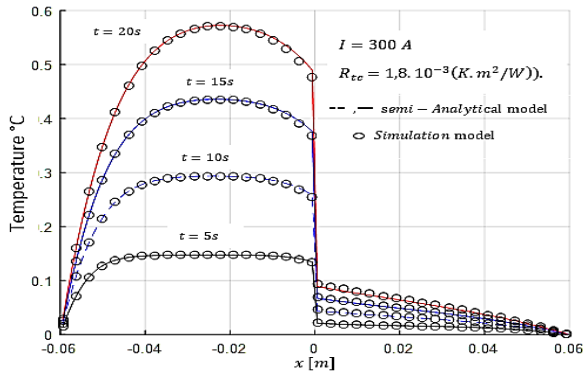> **Heating due to volumetric powers with finite lengths**

Figure 2. Temperature fields related to volumetric powers

Figure 2 provides a comparative analysis of the temperature fields generated by the flow using two different approaches: The semi-analytical method and the COMSOL simulation model. The simulation is performed using the Titanium/Aluminium material combination, with a generated flow intensity of 2000 W/m² and a partition coefficient α of 0.7. The contact resistance is assumed to be $Rtc=1.8\times10^{-3}$ ($K.m^2/W$). At various time intervals, the temperature distribution patterns are examined.

At $t=2s$, a notable difference is observed between the penetration depths of the temperature fields in aluminium and titanium. The penetration depth reaches 40mm in aluminium, indicating efficient heat propagation and response. On the other hand, the penetration depth in titanium is less than 20mm, suggesting a slower response to heat propagation compared to aluminium. This discrepancy can be attributed to the contrasting thermal conductivities and diffusivities of the two materials.

It is important to consider that the hypothesis of semi-infinite media is valid only for $t<0.15\tau$ [15, 16], where, τ represents the fundamental time constant. This time constant is derived from the transcendental equation solved using the separation of variables method [22]. The implication is that the semi-analytical approach provides accurate results within the specified time range, while the COMSOL simulation model offers a comprehensive and detailed analysis of the temperature fields.

> **Case 2: Heating due to the generated flow**

3.1 Generated flow (infinite lengths)

Figure 3 depicts a detailed comparison of the short-term temperature changes between the Comsol simulation model and the semi-analytical model. Notably, in the aluminium bar at point $x_2=2$ mm, the temperature difference between the two models begins to increase around $t=6$ s. Conversely, in the titanium rod at point $x_1=-2$ mm, the deviation between the two curves is observed at $t=33$ s. These deviations can be attributed to the influence of thermal diffusivity. More specifically, at a given time, a material with higher thermal diffusivity will exhibit a greater depth of temperature penetration compared to a material with lower diffusivity.
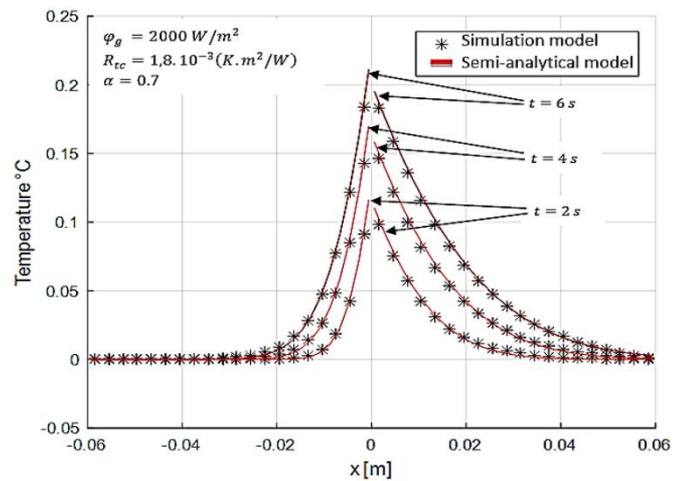
Figure 3. Temperature fields related to generated flow (infinite lengths)

This observation emphasizes that the semi-infinite approximation, which simplifies calculations by eliminating two constants (as x approaches $\pm\infty$), has limited convergence for materials with higher thermal diffusivity. As highlighted in Figure 4, the semi-analytical solution is valid only for $t\leq6s$ in Aluminium, while the method of separating variables converges beyond $r=78s$ in the same case.
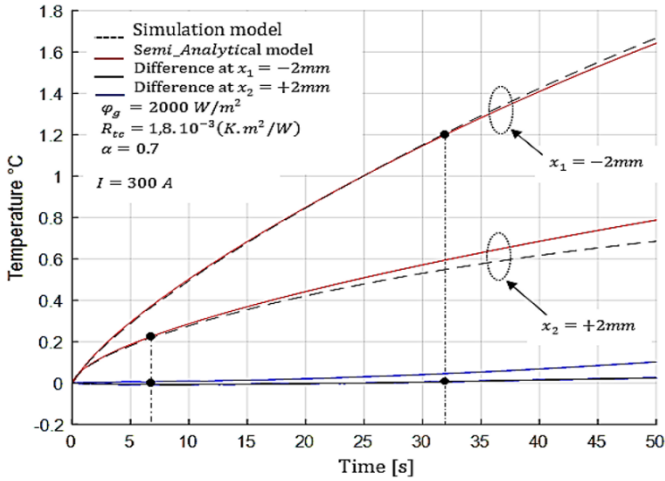

Figure 4. Comparison between the simulation model and the semi-analytic model in short time

3.2 Generated flow (finite lengths)

To overcome these limitations and obtain more accurate results, it is proposed to solve the 'D' system using the Laplace method. This approach provides a more robust representation of the heating related to the flow generated in transitional mode at finite lengths.
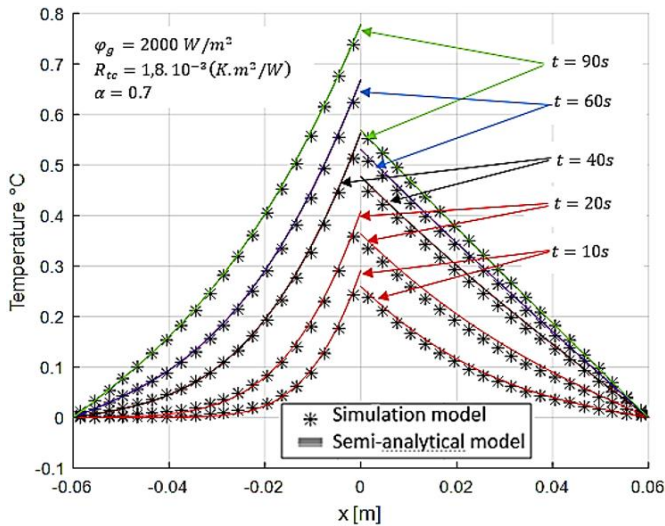

Figure 5. Temperature fields related to generated Flow (finite Lengths)

Figure 5 provides a detailed comparison between the temperature profiles obtained from the semi-analytical model and the finite length model at different time intervals. The finite length model takes into account the boundaries of the system at shorter times (up to approximately 6 seconds). It can be observed that the resolution at finite lengths demonstrates a longer convergence time compared to the previous method. This is particularly relevant when considering situations where

imposed lengths are present, which closely resemble real-world scenarios.

The incorporation of the Laplace method in our semi-analytical model for electrothermal modeling unveils crucial nuances in the transient behavior of materials. Figures 3 and 4 highlight the limitations of the case "Generated Flow (Infinite Lengths)," showcasing a notable divergence from Comsol simulations, particularly for highly diffusive materials like aluminum.

The introduction of finite lengths in the case "Generated Flow (Finite Lengths)", coupled with the Laplace method, demonstrates enhanced convergence. This adaptation proves essential, providing a more robust representation of transient thermal behavior. Extending simulations up to $t=90s$ strengthens the reliability of our approach and underscores the relevance of the Laplace method in modeling thermal transitions.

This emphasizes the significance of employing techniques such as the Laplace method to address complexities associated with imposed lengths, ensuring dependable outcomes in practical electrothermal applications.

4. CONCLUSIONS

Electrothermal phenomena play a crucial role in numerous industrial applications, where the interaction between electricity and heat transfer is of paramount importance. The study of electrothermal processes aims to understand the complex interplay between electrical currents and thermal effects, enabling the development of efficient and reliable systems.

This work investigates the problem of electrothermal contact, with a focus on heat conduction during short time intervals. Specifically, it develops an analytical approach to solve the direct problem of heat conduction in electrothermal contacts, taking into consideration the dissipation of heat due to Joule heating. This aspect has received limited attention in the existing literature, indicating the need for further investigation.

Additionally, a semi-analytical model is employed, combining analytical techniques with numerical methods to provide a robust and accurate description of the heat transfer process. The model is validated and tested using the Comsol software, which enables comprehensive simulations and analysis of electrothermal contact phenomena.

- ➢ The investigation of electrothermal contact phenomena, focusing on short time intervals, has provided valuable insights for industrial applications such as electric resistance spot welding.
- ➢ The semi-analytical method used in this study shows convergence at short times for more diffuse materials like Titanium and Aluminum.
- ➢ The depth of penetration and temperature changes can be accurately predicted within a time frame of 6 seconds for Aluminum.
- ➢ For Titanium, the convergence of the semi-analytical method occurs at longer times, around 33 seconds, due to differences in thermal diffusivity.
- ➢ Considering finite lengths in the modeling approach provides additional insights into the heat transfer process.
- ➢ The model converges for both short and long times,

regardless of the material's diffusivity, when finite lengths are considered.

> The implications of these findings are significant for electric resistance spot welding, as engineers can optimize welding parameters for both Titanium and Aluminum.

> Understanding the different thermal behaviors of these materials allows for precise control over the welding process.

> The limitations of the semi-infinite assumption in modeling have been identified, emphasizing the importance of considering finite lengths for accurate temperature predictions.

The validated semi-analytical model presents potential as a direct tool for determining key parameters governing electrothermal contacts. It can play a crucial role in experimental studies aimed at identifying and characterizing critical factors such as the partition coefficient, thermal resistance, and electrical resistance in electrothermal contacts. This potential application opens avenues for more targeted and informed experimental investigations, fostering a deeper understanding of underlying mechanisms and providing a foundation for optimizing the design and performance of electrothermal contact devices and systems. In the future, research could focus on utilizing the validated semi-analytical model to extract practical parameters, bridging the gap between theoretical knowledge and real-world applications. This approach has the potential to enhance the accuracy and applicability of electrothermal contact modeling in various industrial contexts.

ACKNOWLEDGMENT

REFERENCES

[1] Umbricht, G.F., Rubio, D., Tarzia, D.A. (2021). Estimation of a thermal conductivity in a stationary heat transfer problem with a solid-solid interface. International Journal of Heat and Technology, 39(2): 337-344. https://doi.org/10.18280/ijht.390202

[2] Umbricht, G.F., Tarzia, D.A., Rubio, D. (2022). Determination of two homogeneous materials in a bar with solid-solid interface. Mathematical Modelling of Engineering Problems, 9(3): 568-576. https://doi.org/10.18280/mmep.090302

[3] Zemmouri, A., Azzouz, S., Benchadli, D., Ayad, A., Chaoui, K. (2023). Study of the periodic thermal contact between exhaust valve and its seat in an internal combustion engine. Eksploatacja i Niezawodność - Maintenance and Reliability, 25(2): 162911. https://doi.org/10.17531/ein/162911

[4] Bouhadjela, F., Bensaad, B., Cheriet, R., Belharizi, M., Belhenini, S. (2020). Contribution to the study of plastic mechanics models of solid-solid contacts. Annales de Chimie - Science des Matériaux, 44(1): 37-42. https://doi.org/10.18280/acsm.440105

[5] Cheriet, R., Bensaad, B., Bouhadjela, F., Belhenini, S., Belharizi, M. (2021). Contribution to the study of solid-solid thermal contact resistances--A comparative study. Annales de Chimie - Science des Matériaux, 45(4): 267-272. https://doi.org/10.18280/acsm.450401

[6] Rachid, C., Lebon, F., Rosu, I., Mohammed, M. (2019). Numerical study of the surface roughness, thermal conductivity of the contact materials and interstitial fluid convection coefficient effect on the thermal contact conductance. Annales de Chimie: Science des Materiaux, 43(4): 265-271. https://doi.org/10.18280/acsm.430410

[7] Touati, S., Mekhilef, S. (2017). Statistical analysis of surface roughness in turning based on cutting parameters and tool vibrations with response surface methodology (RSM). Materiaux et Techniques, 105(4): 401. https://doi.org/10.1051/mattech/2017037

[8] Touati, S., Ghelani, L., Zemmouri, A., Boumediri, H. (2022). Optimization of gas carburizing treatment parameters of low carbon steel using Taguchi and grey relational analysis (TA-GRA). International Journal of Advanced Manufacturing Technology, 120(11-12): 7937-7949. https://doi.org/10.1007/s00170-022-09302-0

[9] Azzouz, S., Bourouga, B., Chaoui, K. (2007). Transfert thermique a travers une interface de contact intermittent en regime periodique etabli. Revue Synthèse, 16: 102-108.

[10] Murugesan, V., Varthanan, P.A., Murugan, S.S., Gokilakrishnan, G. (2022). Numerical analysis of the effect of heat input in the spot welding of dissimilar materials. Materials and Technology, 56(3): 307-313. https://doi.org/10.17222/mit.2022.411

[11] Pashazadeh, H., Gheisari, Y., Hamedi, M. (2016). Statistical modeling and optimization of resistance spot welding process parameters using neural networks and multi-objective genetic algorithm. Journal of Intelligent Manufacturing, 27(3): 549-559. https://doi.org/10.1007/s10845-014-0891-x

[12] Feulvarch, E., Robin, V., Bergheau, J.M. (2004). Resistance spot welding simulation: A general finite element formulation of electrothermal contact conditions. Journal of Materials Processing Technology, 153-154(1-3): 436-441. https://doi.org/10.1016/j.jmatprotec.2004.04.096

[13] Le Meur, G., Bourouga, B., Dupuy, T. (2003). Measurement of contact parameters at electrode/sheet interface during resistance spot welding process. Science and Technology of Welding and Joining, 8(6): 415-422. https://doi.org/10.1179/136217103225005589

[14] Le Meur, G., Bourouga, B., Bardon, J.P. (2006). Microscopic analysis of interfacial electrothermal phenomena -- Definition of a heat generation factor. International Journal of Heat and Mass Transfer, 49(1-2): 387-401. https://doi.org/10.1016/j.ijheatmasstransfer.2005.02.029

[15] Mokrani, H., Bourouga, B. (2007). Mesure des paramètres de contact à une interface de contact électrothermique imparfait. Congrès Français de Thermique, SFT 2007, Ile des Embiez, 1-6. https://www.sft.asso.fr/Local/sft/dir/user-3775/documents/actes/Congres_2007/communications/426.pdf.

[16] Mokrani, H., Fadda, H., Bourouga, B., Azzouz, S.,

Chaoui, K. (2013). Etude expérimentale du contact électrothermique imparfait à une interface métal-métal. Journées Internationales de Thermique, Marrakech.

[17] Degiovanni, A., Jannot, Y., Moyne, C. (2022). Electrical analogy associated with a multi-isotherms medium with internal heat source. Thermal Science and Engineering Progress, 28: 1-26. https://doi.org/10.1016/J.TSEP.2021.101177

[18] El Maakoul, A., Moyne, C., Degiovanni, A. (2019). A general approach to solve heat conduction problems with internal heat sources using resistance and quadrupole concepts. International Journal of Heat and Mass Transfer, 129: 793-800, https://doi.org/10.1016/j.ijheatmasstransfer.2018.10.008

[19] El Maakoul, A., Remy, B., Degiovanni, A. (2019). Modeling of thermal contacts with heat generation: Application to electrothermal problems. International Journal of Heat and Mass Transfer, 140: 293-302. https://doi.org/10.1016/j.ijheatmasstransfer.2019.06.015

[20] Stehfest, H. (1970). Numerical inversion of Laplace transforms. Communications of the ACM, 13(1): 47-49. https://doi.org/10.1145/361953.361969

[21] Yovanovich, M.M. (1981). New contact and gap correlations for conforming rough surfaces. In AIAA 16th Thermophysics Coference, (AIAA Paper No. 81-1164) (ed): Palo Alto, CA: 1981.

[22] Pishkoo, A., Darus, M., Tamizi, F. (2014). A solution of fractional Laplace's equation by modified separation of variables. Journal of Advances in Physics, 4(1): 397-403. https://doi.org/10.24297/jap.v4i1.2049